Quantitative force and dissipation measurements in liquids using piezo-excited atomic force microscopy: a unifying theory

2011 Nanotechnology 22 485502

(http://iopscience.iop.org/0957-4484/22/48/485502)

Nanotechnology **22** (2011) 485502 (11pp) doi:10.1088/0957-4484/22/48/485502

Quantitative force and dissipation measurements in liquids using piezo-excited atomic force microscopy: a unifying theory

Daniel Kiracofe and Arvind Raman

Birck Nanotechnology Center and School of Mechanical Engineering, Purdue University, West Lafayette, IN 47907, USA

Received 11 August 2011, in final form 29 September 2011
Published 9 November 2011
Online at stacks.iop.org/Nano/22/485502

Abstract

The use of a piezoelectric element (acoustic excitation) to vibrate the base of microcantilevers is a popular method for dynamic atomic force microscopy. In air or vacuum, the base motion is so small (relative to tip motion) that it can be neglected. However, in liquid environments the base motion can be large and cannot be neglected. Yet it cannot be directly observed in most AFMs. Therefore, in liquids, quantitative force and energy dissipation spectroscopy with acoustic AFM relies on theoretical formulae and models to estimate the magnitude of the base motion. However, such formulae can be inaccurate due to several effects. For example, a significant component of the piezo excitation does not mechanically excite the cantilever but rather transmits acoustic waves through the surrounding liquid, which in turn indirectly excites the cantilever. Moreover, resonances of the piezo, chip and holder can obscure the true cantilever dynamics even in well-designed liquid cells. Although some groups have tried to overcome these limitations (either by theory modification or better design of piezos and liquid cells), it is generally accepted that acoustic excitation is unsuitable for quantitative force and dissipation spectroscopy in liquids. In this paper the authors present a careful study of the base motion and excitation forces and propose a method by which quantitative analysis is in fact possible, thus opening this popular method for quantitative force and dissipation spectroscopy using dynamic AFM in liquids. This method is validated by experiments in water on mica using a scanning laser Doppler vibrometer, which can measure the actual base motion. Finally, the method is demonstrated by using small-amplitude dynamic AFM to extract the force gradients and dissipation on solvation shells of octamethylcyclotetrasiloxane (OMCTS) molecules on mica.

S Online supplementary data available from stacks.iop.org/Nano/22/485502/mmedia

(Some figures may appear in colour only in the online journal)

1. Introduction

1.1. Background

One of the great accomplishments of dynamic atomic force microscopy (dAFM) methods is their ability to quantify the local force gradients and energy dissipation that act between the nanoscale tip of the AFM probe and the sample. This allows the determination of surface and material properties at the nanoscale and is of great interest to researchers in a wide variety of disciplines.

One popular excitation method for dynamic AFM is the so-called acoustic method, which uses a dither piezoelectric element to mechanically vibrate the base of the cantilever. It is well known that the piezo excitation spectrum in liquids is filled with many apparent resonance peaks that are not related to the cantilever resonance, which was first recognized in [1]. This obscures the true cantilever dynamics and makes

it difficult to determine the cantilever natural frequency and quality factor, even in well-designed fluid cells.

Despite its known problems, many research groups still use piezo excitation in liquids and it comes standard on nearly all commercial AFMs. The reasons for its continued popularity may include the fact that the alternatives, such as magnetic [2], Lorentz force [3] or photothermal excitation [4], are more complicated and expensive. Thus, there would be significant interest in a conclusive demonstration of quantitative force and dissipation spectroscopy in liquids using piezo-excited AFM. Some groups have attempted to perform quantitative spectroscopy in piezo mode with mixed success [5, 6] and others have attempted to design custom fluid cells to reduce the spurious resonances [7–10]. However, the general consensus is that quantitative force or dissipation spectroscopy using piezo mode in liquids remains difficult.

However, there is a much larger problem with acoustic excitation in liquids that is often overlooked. This is the problem of large base motion. The base motion cannot be directly observed in typical AFMs that use the optical beam deflection method. In air or vacuum environments, base motion is negligibly small compared to the tip motion. Therefore, the lack of knowledge of the base motion is not an obstacle to quantitative measurements. However, in liquid environments, base motion can be large [11–13]. Further, the observed cantilever amplitude and phase are strongly affected by non-resonant interactions due to the base motion in addition to the classic resonant detuning effects ([11, 5] and explained in more detail in section 1.2.2). This problem of large, unknown base motion exists regardless of the presence or absence of piezo resonances, and would still be present even if the 'forest of peaks' [1] were completely eliminated. Therefore, any quantitative analysis for acoustic excitation in liquids must use some theoretical formula or model to estimate the magnitude of the unknown base motion.

A routine assumption is that the base motion is related to the amplitude at resonance by the quality factor, e.g. $A_0 \approx YQ$, where A_0 is the initial tip amplitude, Y is the base motion and Q is the quality factor. Standard formulae for force spectroscopy using piezo excitation include these assumptions [11, 5]. Despite the fact that these assumptions are critical to obtaining quantitative results, they have never been tested experimentally.

The intent of this work, then, is to experimentally test these commonly used assumptions. The layout of this paper is as follows: first we will review some of the current commonly applied formulae and point out some common problems with them. Then, using a scanning laser Doppler vibrometer, we directly measure a cantilever's base motion and demonstrate that current models generally greatly over-predict the base motion (often >100% error). Then we present a new, more accurate model. A key feature of this model is that it includes two distinct components of excitation forces—a structure-borne excitation (i.e. mechanical excitation from the base motion) and a fluid-borne excitation (i.e. vibration transmitted to the surrounding liquid from the vibrating piezo which then applies an oscillating force to the cantilever). The fluid-borne excitation forces are important in a liquid environment as they are often of the same order as the structure-borne forces. The fluid-borne excitation forces have been recognized before [13–15], but previously there was no method to separate the two components in an experimental measurement. The central contribution of this work is a simple method to distinguish these two different types of excitation, thereby leading to accurate estimates of the base motion which in turn leads to accurate spectroscopy formulae. These estimates can be performed on any AFM and do not require any additional hardware. This method is validated experimentally. Finally, we develop force spectroscopy equations that take both types of excitation into account, and then demonstrate use of the method on the oscillatory forces of octamethylcyclotetrasiloxane (OMCTS) over mica using small-amplitude dynamic AFM.

1.2. Common mistakes in using standard formulae for force and dissipation spectroscopy using piezo excitation in liquids

In this section, we review some of the commonly used standard AFM formulae. Many AFM researchers use these formulae without recognizing some of the assumptions regarding base motion that are made in their derivation. Therefore, the goal in this section is to point out those assumptions explicitly and show where they break down in liquid environments. This will then serve to motivate the further study of piezo excitation in liquids.

1.2.1. Review of equations for air/vacuum. First, we review the formulae for air/vacuum for later comparison. In the event that the amplitude is small (compared to some length scale of the interaction force) and the excitation frequency is near the jth natural frequency, the governing differential equation of an AFM cantilever is often approximated by the linear point-mass model

$$\frac{\ddot{q}(t)}{\omega_j^2} + \frac{\dot{q}(t)}{\omega_j Q_j} + q(t) = \frac{k_{\text{int}} q(t) + \gamma \dot{q}(t)}{k_j} + \frac{F_{\text{drive}} \cos \omega t}{k_j} \quad (1)$$

where q, ω, ω_j, k_j, k_{int}, γ, Q_j and F_{drive} are the cantilever deflection, driving frequency, natural frequency, equivalent modal stiffness, sample stiffness, sample damping coefficient, quality factor and driving force, respectively. This equation can be solved for the response amplitude and phase and then inverted to give the linear AM-AFM force spectroscopy formula [16]

$$k_{\text{int}} = k_j \left(\frac{\omega^2}{\omega_j^2} - 1 + \frac{A_0 \cos \phi}{AQ} \right) \quad (2)$$

where A, ϕ and A_0 are the first harmonic amplitude, first harmonic phase and unconstrained (initial) amplitude, respectively. A similar formula exists to find γ. In air or vacuum; (2) is applicable regardless of the method of excitation.

1.2.2. Typical point-mass models used in liquid environments. Several authors have recognized that, in liquid environments, the choice of excitation matters. Specifically, in acoustic

excitation the total tip motion is the sum of cantilever deflection q and base motion Y. Base motion can be quite large in liquids. Equation (1) is then modified to be

$$\frac{\ddot{q}(t)}{\omega_j^2} + \frac{\dot{q}(t)}{\omega_j Q_j} + q(t) = \frac{k_{\text{int}}\left(Y(t)+q(t)\right) + \gamma\left(\dot{Y}(t)+\dot{q}(t)\right)}{k_j} + \frac{F_{\text{drive}}\cos\omega t}{k_j}. \quad (3)$$

There are two new terms $k_{\text{int}}Y$ and $\gamma\dot{Y}$, which we will refer to as base–sample work terms. These terms represent the fact that the base motion creates a tip–sample interaction force, which in turn can cause a motion of the tip $q(t)$. In other words, even if $F_{\text{drive}} = 0$, an oscillating motion of Y in the presence of a sample will cause an oscillating motion of q. The observed amplitude and phase will thus be modified by the base–sample work, which is not accounted for by (2). A common extension of (2) to account for the base–sample work is [11, 5]

$$k_{\text{int}} = k_j\left(\frac{\omega^2}{\omega_j^2} - 1 + \frac{Y(Y + A\cos\phi)}{Y^2 + A^2 + 2YA\cos\phi}\right). \quad (4)$$

However, the base motion Y cannot be directly observed using the optical beam deflection method, it must be estimated using some model of the cantilever dynamics. The typical ad hoc point-mass model theory gives

$$\frac{A_0(\omega)e^{i\phi_0(\omega)}}{Y(\omega)} = \frac{(\omega^2 - i\frac{\omega\omega_j}{Q_j})}{\omega_j^2 + i\frac{\omega\omega_j}{Q_j} - \omega^2}. \quad (5)$$

For the case $\omega = \omega_j$, the magnitudes in (5) reduce to

$$|Y| = \frac{A_0}{\sqrt{1+Q_j^2}}. \quad (6)$$

Equation (5) can be combined with (4) to yield [11, 5]

$$k_{\text{int}} = k_j\left(\frac{\omega^2}{\omega_j^2} - 1 + \frac{A_0}{A}\times\left(\frac{\cos\phi + A_0/A\sqrt{1+Q_j^2}}{\sqrt{1+Q_j^2} + (2A_0\cos\phi)/A + A_0^2/(A^2\sqrt{1+Q_j^2})}\right)\right) \quad (7)$$

Another common formula in AM-AFM is the energy dissipation formula [17], which can be written in this form:

$$P = \frac{1}{2}\frac{k_j\omega}{Q_j}\left(A_0 A\sin\phi - A^2\frac{\omega}{\omega_j}\right). \quad (8)$$

This equation assumes $A_0 = YQ_j$, which is an approximation to (6) valid for high Q.

1.2.3. The continuous beam theory. There are several problems with the approach of section 1.2.2. First, (5) and (6) are derived from a model of a point-mass oscillator and neglect the continuous nature of the cantilever beam. Using Euler–Bernoulli beam theory to take into account the shape of the eigenmode yields (for $\omega = \omega_j$) [18, 13]:

$$|Y| = \frac{\int_0^L \psi_j^2(x)\,dx}{\int_0^L \psi_j(x)\,dx}\frac{A_0}{\sqrt{1+Q_j^2}} = \frac{\alpha_j}{\beta_j}\frac{A_0}{\sqrt{1+Q_j^2}} \quad (9)$$

where $\psi_j(x)$ is the jth eigenmode shape and L is the length of the beam. A complete derivation of this equation can be found in the supplementary information (available at stacks.iop.org/Nano/22/485502/mmedia). The values of α_j/β_j for $j = 1\cdots4$ are 0.639, −1.15, 1.97 and −2.75. There are two things to note: first, the values are different for different eigenmodes, which means that the ratio between base motion and tip motion must be different for different eigenmodes[1], but (6) treats all eigenmodes the same. Second, for some eigenmodes, α_j/β_j is positive, but for others it is negative. This indicates a phase difference between tip and base. For example, for $\omega < \omega_j$, positive α_j/β_j means that, when the base moves up, the tip moves up. Negative α_j/β_j means that when the base moves up the tip moves down. For this reason the ad hoc point-mass model (6) and the resulting formula equation (7) can be quite inaccurate.

1.2.4. Frequency modulation force spectroscopy. Other types of dynamic AFM have their own standard formulae, which also have similar problems regarding base motion. For example, in (1), a change in k_{int} will cause a change in the natural frequency of the oscillator, which in turn causes a shift in phase. Therefore FM-AFM uses a feedback loop to change the driving frequency to keep phase constant, thus keeping the driving frequency equal to the natural frequency. However, from (3), it is clear that, with acoustic excitation, a change in k_{int} will also cause a change in the phase due to the $k_{\text{int}}Y$ term. Therefore, in liquids, keeping phase constant does not necessarily keep the driving frequency fixed at the natural frequency. FM-AFM formulae that calculate k_{int} based on the driving frequency such as [21] will thus be in error.

1.2.5. Motivation for the present work. In air or vacuum, $Q \gg 1$, so that $Y \ll A_0$. Therefore calculating the base motion incorrectly or even neglecting it completely does not significantly affect most calculations. However, in liquids, Q is typically in the range of 1–6, such that Y is of the same order as A_0. Therefore it is important to calculate it correctly. A natural question to ask is: does (9) still hold in liquids? Many authors have assumed that it does, but to our knowledge, this has never been tested experimentally.

We will show in this paper that the use of (9) or the ad hoc (5) in liquids leads to significant errors in the base motion magnitude, which in turns leads to major errors in force and dissipation spectroscopy. We then propose an experimental protocol coupled with theoretical modeling that does allow an experimentalist to correctly identify the magnitude of base motion and correctly measure interaction forces and dissipation in piezo-excited AFM in liquids.

[1] Strictly speaking, β and α can be altered by the presence of a tip mass on the end of the cantilever, but for liquids this effect is weak [19, 20].

2. Experimental measurement of base motion in liquids using laser Doppler vibrometer

Typical AFMs using the optical beam deflection method with photodiodes actually measure the slope of the cantilever, not the actual deflection. Because a cantilever has zero slope at its base, typical AFMs are not able to measure the base motion. To directly measure the base motion in liquids we use a scanning laser Doppler vibrometer (LDV) (MSA-400, Polytec, Waldbronn Germany, typical laser spot 1–2 μm). The LDV measures the Doppler shift of laser light which is reflected off a surface, and thus is able to directly measure the velocity of any point on the cantilever. For this experiment, a Mikromasch NSC36 cantilever is attached to a piezo in a custom-built liquid cell. The experimental set-up is shown in figure 1(a) and is similar to that used in [19].

To test the theoretical models for base motion described in section 1.2, we measure both the tip motion and base motion over a range of frequencies. The result is shown in figures 1(b) and (c). The raw data shows many peaks, which correspond to piezo or liquid cell resonances. Note that these peaks occur in both the tip motion and base motion—therefore the base motion is *not* constant with frequency, as has been assumed in some prior literature [13]. However, when the relative tip motion (tip–base) is divided by the base motion, a clean cantilever resonance peak is obtained (figure 1(d)).

The experimental data is curve-fitted (least squares) to the theoretical models given in section 1.2.5. Specifically, for the line labeled 'point-mass model', the right-hand side of equation (5) is curve-fitted to the data with ω_1 and Q_1 as the two fitting parameters. Both the experimental data and equation (5) were normalized to unity magnitude at resonant before the fit[2]. The same procedure is followed for the line labeled 'Ideal beam model', except α_j/β_j is included.

The model of equation (9) clearly does not match the experiment. Specifically, although the shape of the curve matches well, the magnitude at resonance is off by nearly a factor of two. This will directly lead to errors in force spectroscopy formulae. It is important to note that such errors would still be present even if all piezo resonances could be removed by redesigning the piezo/liquid cell. Further, equation (9) does not depend on stiffness, so simply increasing the cantilever stiffness will not eliminate the problem (however, stiff commercial cantilevers typically have a somewhat higher quality factor than soft ones, which does reduce the problem).

Therefore, we can conclude that (9) does not hold, in general, in liquids. In particular, in figure 1, the cantilever base is moving 40% less than expected from (9) for the observed tip motion. How is this possible? The logical conclusion is that there must be some other additional driving force, which is moving the cantilever tip but not its base. We explore this idea in section 3.1.

[2] This normalization allows the curve fitting to match the location and width of the peak correctly without regard to the height of the peak. Without normalization, the curve fit may overestimate the quality factor in order to match the peak height correctly. This is because the point-mass model has only two free parameters and thus the three quantities (location, width and height of the peak) cannot all be fitted simultaneously.

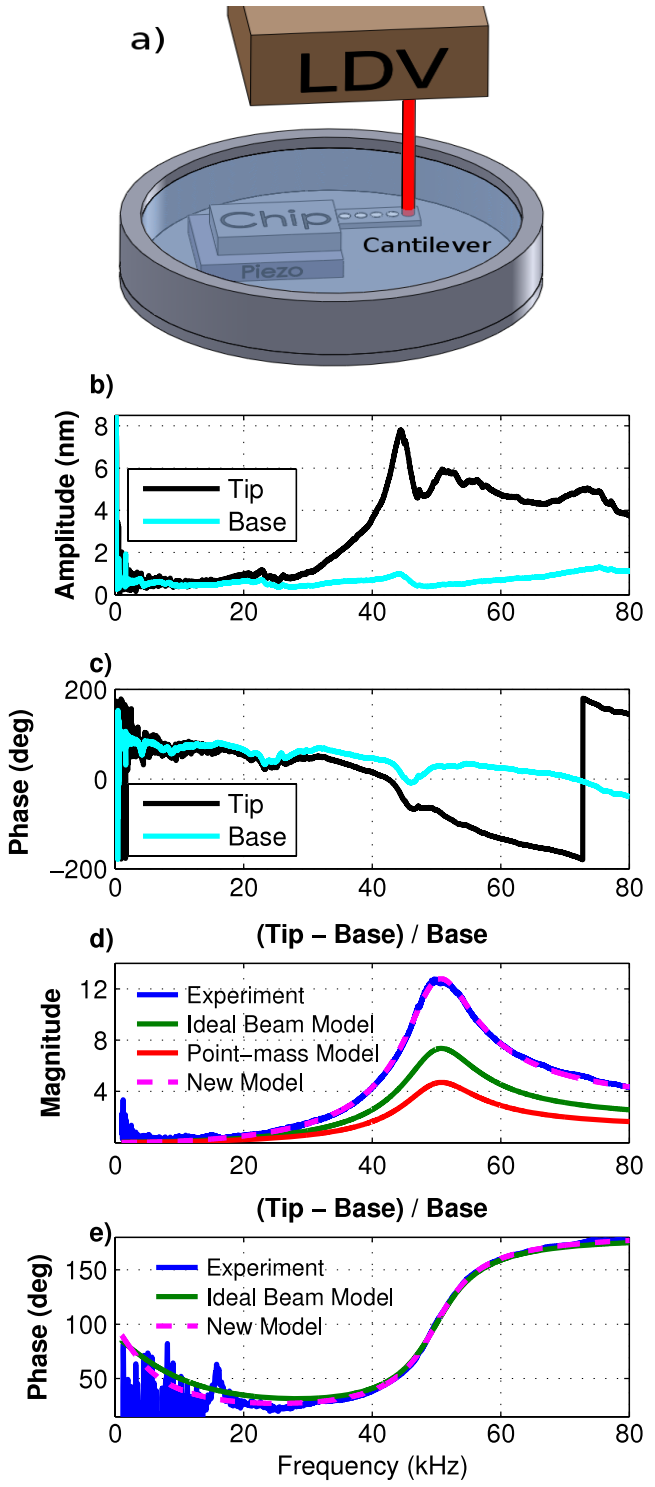

Figure 1. Experimental piezo-driven frequency sweep of a cantilever in water far from any surface. (a) Schematic of set-up: a scanning laser Doppler vibrometer is used to measure motion at multiple points along the cantilever, including tip and base. The raw data ((b) amplitude and (c) phase) shows many peaks indicating piezo resonances. Dividing the (relative) tip motion by the base motion reveals the underlying cantilever transfer function ((d) amplitude and (e) phase). The ideal beam model (9) has an amplitude error of 70% and the point-mass model (6) has an amplitude error of 167%. In contrast, the new model given in section 3.1 fits the data nearly exactly. All of the models fit the phase well, although the new model is slightly better below resonance. (In (e), point-mass model gives the same phase as ideal beam model and thus is not shown.)

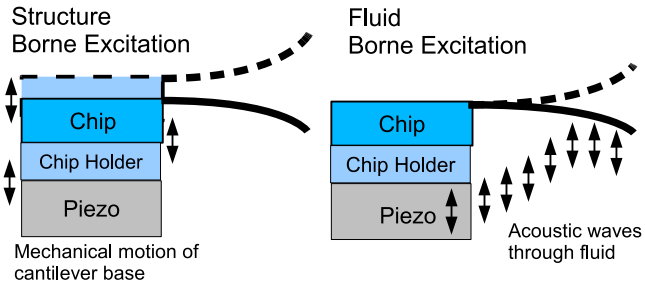

Figure 2. There are two different types of excitation caused by the dither piezo in liquids. First, extension and contraction of the piezo crystal causes the base of the cantilever (i.e. the chip) to move up and down. Because of inertial and fluid forces, the cantilever bends when the base is displaced. Second, acoustic waves travel from the piezo through the liquid and excite the cantilever directly. The total excitation on the cantilever is a linear combination of these two types of excitation.

3. Proposed theory

3.1. The fluid-borne excitation force

We have demonstrated that the base motion and tip motion in liquids are not related by (9) and that there must be some additional force driving the cantilever, which is yet to be identified. A potential candidate for this force is the unsteady motion of the liquid in the cell, which in turn is generated by the vibrating piezo. Such a fluid forcing has been postulated by several authors before [13, 14, 22, 15]. We will refer to this excitation as 'fluid-borne excitation', in contrast to the mechanical excitation of the cantilever base, which will be referred to as 'structure-borne excitation'. These two different excitations are illustrated schematically in figure 2.

The most general description is due to [13], who makes the following two assumptions. First, both the structure-borne excitation and fluid-borne excitation are generated by the vibrating piezo. Therefore, we assume that both the oscillating base motion and the oscillating local flow velocity around the cantilever are linearly proportional to the piezo motion. Second, the oscillating flow velocity is assumed to be approximately constant along the length of the cantilever, allowing the use of the hydrodynamic function to describe the forces [23, 24]. With these assumptions, it can be shown (see supplementary information available at stacks.iop.org/Nano/22/485502/mmedia) that the complex transfer function relating the amplitude and phase of the tip motion to the base motion, when corrected for the forcing from unsteady liquid motion, is

$$\frac{A_0(\omega)e^{i\phi_0(\omega)}}{Y(\omega)} = \frac{\beta_j}{\alpha_j}\frac{(\omega^2 - i\frac{\omega\omega_j}{Q_j})(1 + A_{\text{fluid}}(\omega))}{\omega_j^2 + i\frac{\omega\omega_j}{Q_j} - \omega^2} \qquad (10)$$

where A_0 and ϕ_0 are the unconstrained amplitude and phase, and A_{fluid} is a dimensionless complex constant indicating the relative magnitude of the fluid-borne to structure-borne excitation. Note (10) is valid only for drive frequencies within the cantilever resonance bandwidth. For drive frequencies outside this range, multiple eigenmodes may respond and the full frequency-dependent hydrodynamic function must be included instead of just using a quality factor Q_j.

The two limiting cases are $A_{\text{fluid}} \to 0$, in which the structure-borne-only formula (9) is recovered, and $A_{\text{fluid}} \to \infty$, which implies $Y \to 0$ and leads to fluid-borne excitation only (similar to the models of [14, 15]). Thus, this unifying model is sufficiently general to capture the behavior of all previous models.

We now apply the above theory to the data presented in figure 1. A least-squares fit of (10) to the data gives a value of A_{fluid} of $0.92 + 0.013i$, which fits the data nearly exactly[3]. This confirms the hypothesis that fluid motion is responsible for the additional forcing. The value $0.92 + 0.013i$ should be interpreted as indicating that the fluid-borne excitation forces are about the same magnitude as the structure-borne excitation and are approximately in-phase with the structure-borne excitation. This means that, by neglecting the fluid-borne forces, the previous model was neglecting almost half of the total excitation force applied to the cantilever. This now explains why the previous theory's prediction of base motion was off by nearly a factor of two.

Thus far we have proved by direct LDV measurement of base and tip motion in liquids that the fluid-borne forcing A_{fluid} is significant. Is it possible to easily determine A_{fluid} in a commercial AFM with a photodiode where base motion cannot be directly measured? We address this topic in section 3.2.

3.2. Proposed method to quantitatively determine the fluid-borne excitation and base motion

As previously mentioned, the base motion cannot be directly observed with typical AFMs. However, when a cantilever is in permanent contact with a stiff sample such as mica, the tip is not moving up and down (the indentation is small because the sample is stiff), but the cantilever is still flexing due to the base motion. Because the optical beam deflection method measures the slope at the free end of the cantilever, there is still some measured motion [25], which we refer to as the residual amplitude A_{res} and phase ϕ_{res}. Some authors [13] have suggested that $A_{\text{res}} \approx Y$ and thus used A_{res} to measure Y (and then A_{fluid}). In fact, the fluid-borne excitation force still acts even when the tip is in permanent contact. Therefore A_{res} is, in general, a function of both base motion and fluid-borne excitation, so A_{res} cannot be equated to Y.

However, it is possible to determine a procedure to solve for the two unknowns, base motion Y and fluid-borne excitation A_{fluid}, simultaneously. To solve for two unknowns, two known measurements must be made. The first known condition is when the tip is far from the sample, from which we can obtain the initial amplitude A_0 and phase ϕ_0 (sometimes called free/unconstrained amplitude and phase). A second known condition is permanent contact with a stiff sample from which we can obtain the residual amplitude A_{res} and phase ϕ_{res}.

The equation describing the indicated residual motion can be derived (see supplementary information available at stacks.iop.org/Nano/22/485502/mmedia) by assuming that the beam is described by a clamped–pinned boundary condition and does not slip on the surface. For excitation frequencies near the

[3] In this case we assumed A_{fluid} to be constant over the entire frequency range shown, although in general it may be an arbitrary function of frequency.

cantilever's first natural frequency, and assuming that only the first eigenmode responds, the relation is

$$A_{\text{res}}e^{i\phi_{\text{res}}} = \frac{Y}{1.376} \times \left(-5.71\frac{(0.510 + 0.861A_{\text{fluid}})(\omega^2 - \frac{i\omega\omega_1}{Q_1})}{19.23\omega_1^2 + \frac{i\omega\omega_1}{Q_1} - \omega^2} - \frac{3}{2}\right). \quad (11)$$

A general formula for higher eigenmodes is in the supplementary information (available at stacks.iop.org/Nano/22/485502/mmedia). The procedure to determine Y and A_{fluid} from measurements of free and residual motion is as follows.

(i) Acquire a thermally driven spectrum and determine the cantilever's natural frequency ω_j and quality factor Q_j from it using a curve-fitting procedure (details in section 6.1).
(ii) Choose a drive frequency ω close to the natural frequency (within the thermal resonance bandwidth). The same drive frequency must be used for the entire experiment. If the drive frequency is changed during the measurement, this process must be repeated at the new frequency.
(iii) Perform a tapping mode approach curve on a stiff sample[4] and note the initial amplitude/phase A_0, ϕ_0 and residual amplitude/phase A_{res}, ϕ_{res}. The approach curve should be extended in either direction until the amplitude and phase stop changing with Z (e.g. in figure 3, a curve that included only $Z = 5$ to -5 would not capture the initial or residual conditions adequately). As the permanent contact measurement may blunt the tip, researchers may wish to perform this calibration after their measurements.
(iv) Equations (10) and (11) are written using a phase lead convention, so if the instrument uses a phase lag convention, convert ϕ_{res} and ϕ_0 to the phase lead convention[5] (in radians).
(v) Solve (10) and (11) simultaneously to yield the base motion Y and fluid-borne excitation factor A_{fluid}. The most general expression for Y and A_{fluid} in terms of the seven variables $\omega, \omega_i, Q_i, A_{\text{res}}, \phi_{\text{res}}, A_0$, and ϕ_0 is very long so it is not given here. However, these equations can be solved easily numerically once the values of the variables are known.

Computer software to automate steps (iv) and (v) is freely available from [26].

4. Experimental validation of proposed formula by integration of AFM and LDV

We demonstrate this method by directly integrating the laser Doppler vibrometer (LDV) with an AFM. This allows us to directly validate the method proposed in section 3.2. A Nanotec AFM with a liquid cell is placed underneath the LDV. A Veeco OLTESPA cantilever ($k = 1.7$ N m^{-1} nominal, $f = 29$ kHz, $Q = 2.96$) is used in deionized water. The experimental set-up is similar to that used in [27] and is shown in figure 3(a).

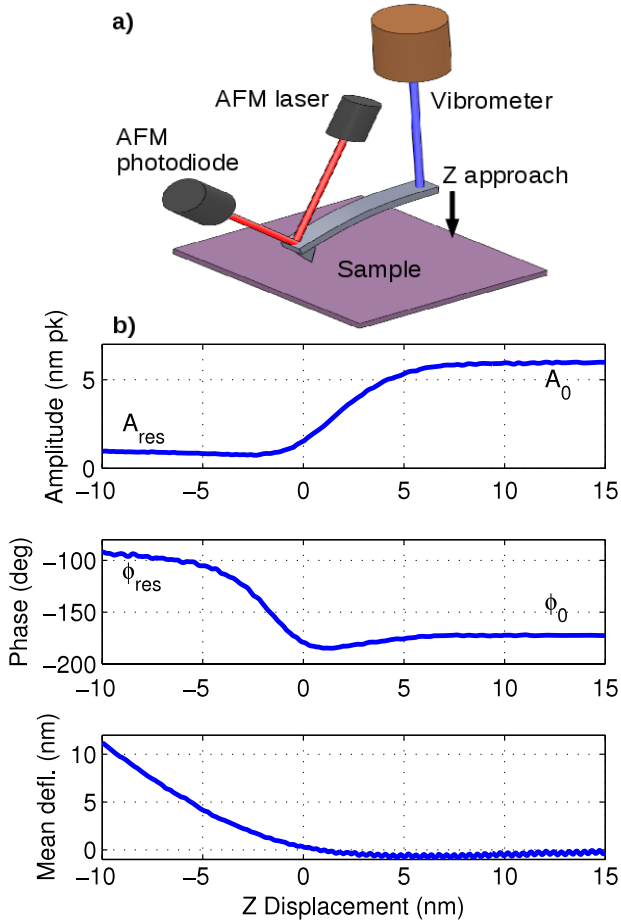

Figure 3. (a) Schematic of experimental set-up. A Nanotec AFM head is placed under a scanning laser Doppler vibrometer. The vibrometer is able to measure both base and tip motion. (b) Dynamic approach curves (tapping mode) for a cantilever on mica in deionized water. The drive frequency, 28.4 kHz, is chosen as the piezo resonance peak closest to the natural frequency, 29.5 kHz. The data has been smoothed to reduce noise. The procedure to calculate base motion from the curve is as follows: first, identify the quantities $A_0, \phi_0, A_{\text{res}}, \phi_{\text{res}}$ at the points labeled on the graph; second, acquire a thermally driven spectrum to obtain the quantities Q_j, ω_j; and finally solve for Y and A_{fluid} in (10) and (11). The result is shown in table 1.

An example dynamic approach curve is shown in figure 3(b). Solving (10) and (11) simultaneously predicts that the magnitude of the (relative) tip motion is 8.6 times the base motion. The predictions of this quantity from previous theories is also calculated. All the quantities are listed in table 1. The proposed theory matches the measurement within about 15%. This error is significantly better than the ideal beam model (error $> 100\%$) and the point-mass model (error $> 200\%$). The calculated value of A_{fluid} for this curve is 0.83–0.18i, or 0.85 at an angle of $-13°$. Again, these fluid-borne excitation forces are about the same magnitude as the structure-borne excitation and are approximately in-phase with the structure-

[4] 'Stiff' is defined relative to the stiffness of the cantilever and the radius of the tip. For cantilevers with $k < 2$ N m^{-1} and typical tip radii of 10 nm or more, mica ($E \approx 60$ GPa) is sufficiently stiff. For stiffer cantilevers, silicon or sapphire would be required.

[5] Phase lead convention means that phase angle decreases as frequency is swept up across resonance and phase lag means phase angle increases as frequency is swept up across resonance.

Table 1. Comparison of measured base and tip motion for the experiment of figure 3 compared against various models. The new model prediction is significantly better than previous models.

		Model predictions (using AFM data)		
	Direct LDV measurement	Point-mass model	Ideal beam model	New model
$\frac{(\text{Tip}-\text{Base})}{\text{Base}}$	9.6	2.9	4.5	8.2
Error $\frac{(\text{Meas.}-\text{Model})}{\text{Model}}$ (%)		231	113	17

borne excitation. An approximately in-phase force is to be expected based on the relatively long acoustic wavelengths compared to the size of the liquid cell [15].

The potential sources of error in the proposed method include:

- It is assumed that the indentation into the stiff calibration sample is zero but in fact there is some non-zero indentation. Note: this assumption implies that the contact resonance frequency is assumed to be equal to the theoretical value of a clamped–pinned beam. Measuring the actual contact resonance frequency could reduce the error in estimating the base motion.
- It is assumed that there is no lateral slipping of the tip when in permanent contact with the calibration sample but the tip may slide a small amount.
- It is assumed that only one eigenmode responds.
- The optical lever sensitivities values used in (11) assume a small laser spot placed near the free end of the cantilever. As the laser spot is moved towards the base, the sensitivity to residual motion decreases, therefore (11) would tend to underestimate base motion. The error is less than 10% provided that the spot is no more than 12% of the length from the free end. There is a similar effect as the spot size increases. The derivation in the supplementary material (available at stacks.iop.org/Nano/22/485502/mmedia) could be corrected for these effects if the size/position is known.
- There may be errors in fitting the thermal response to find Q_j and ω_j.
- There will be some error if the driving frequency is not sufficiently close to the natural frequency of the cantilever (within approximately ω_j/Q_j of the thermal resonance) as discussed in section 3.1.

5. Example quantitative force reconstruction

In section 4, we have shown that the cantilever excitation when using a piezo in liquids is driven by two different forces, the structural-borne excitation, which causes a base motion, and the fluid-borne excitation, which actuates the cantilever directly. We have demonstrated a simple method in which the magnitude of the base motion and fluid-borne excitation can be estimated. Now, with that knowledge, we examine a common force spectroscopy formula (i.e. recovering the physical tip–sample forces from the observed amplitude and phase) and provide a correction to account for the fluid-borne excitation.

5.1. Phase offset

Before giving the force spectroscopy formulae, there is a subtle but important point to address. In a typical AFM, the measured value of phase lag ϕ is not the true cantilever phase lag but includes offsets due to the electronics. In acoustic excitation in particular, there can also be significant phase offsets due to piezo resonances. For $Q \gg 1$, it is known that the true cantilever phase lag away from the sample (ϕ_0) is 90°, so the instrumental phase offsets are compensated for by setting the phase to 90°. However, with acoustic excitation in liquids, ϕ_0 is not necessarily 90°. For example, for $Q_1 = 1.2, \omega = \omega_1$ and $A_{\text{fluid}} = 0$, Equation (10) gives $\phi_0 = 134°$. Thus the typical practice of setting the phase to 90° at the beginning of the experiment is incorrect in liquids with piezo excitation and does not remove the instrumental offsets.

The common force spectroscopy formulae incur significant errors if the instrumental phase offsets are not removed. Specifically, the interaction stiffness and damping will show constant offsets (i.e. they are non-zero far from the sample) and the conservative and dissipative interactions will be coupled [5]. To remove the instrumental phase offsets [11] suggests that the phase should be set to $\cos^{-1}(Q/\sqrt{1+Q^2}) + \pi/2$ for the on-resonance case (and by analogy $\cos^{-1}(-\text{Im}(G)/|G|) + \pi/2$ for the off-resonance case, where G is the right-hand side of (5) and Im means the imaginary part of a complex number). One problem with this is that the cos formulation is only valid for ϕ_0 between 0° and 180°. Simply taking Arg G, where Arg denotes the argument of a complex number (e.g. 'angle' in Matlab) is valid over 0°–360°. The second problem is that (5) neglects the fluid-borne loading and (10) must be used instead. A similar procedure is suggested in [5], but it too neglects fluid-borne loading.

The neglect of fluid-borne loading can be significant. Even modest amounts of fluid-borne excitation can cause (5) to differ from the true phase by a few degrees. For example, the procedure of section 3.2 gives a value of $A_{\text{fluid}} = 0.14 - 0.12\text{i}$ for our Asylum MFD-3D (data not shown). This magnitude is more than four times smaller than the value found in sections 4 or 3.1 for other AFMs, but it is still large enough to cause equation (5) to have a phase error of 8° (for $Q_1 = 1.2, \omega = \omega_1$), which is a large enough offset to cause 35% or more error in the common force spectroscopy formulae. Therefore, accurate knowledge of the fluid-borne loading will still be required to correctly remove instrumental phase offsets, even when the effects on the magnitude of base motion are relatively small.

In the method proposed in this paper, the instrumental phase offsets will cause the calculated value of Y to be a complex-valued quantity. We can remove the phase offsets

by setting the phase of Y to be zero (i.e. purely real) after the calculation[6]. Specifically let Y and ϕ be the experimentally measured quantities (in phase lead convention). Then the adjusted quantities are $\tilde{Y} = |Y|$ and $\tilde{\phi} = \phi - \text{Arg}\, Y$, where $\tilde{\phi}$ is the true cantilever phase with the instrumental offsets removed.

5.2. Small-amplitude (linear) tapping mode formulae

As described in section 1.2, several authors have correctly recognized that the small-amplitude force spectroscopy equations for piezo mode must take into account the base–sample work terms [5, 11]. However, these works have two shortcomings: they generally neglect the continuous nature of the cantilever beam and they neglect fluid-borne excitation. Both of these omissions will result in overestimating the base motion and thus incorrectly reconstructing the tip–sample interaction stiffness and damping. In what follows, we present a formula that correctly accounts for the base motion. The total driving force in the jth eigenmode is

$$F(\omega) = \frac{\tilde{Y} k_j}{\omega_j^2} \frac{\beta_j}{\alpha_j} \left(\omega^2 - \mathrm{i} \frac{\omega_j}{Q_j} \omega \right) (1 + A_{\text{fluid}}). \tag{12}$$

From this, the formula taking into account the base motion and fluid-borne excitation is (see supplementary information for derivation available at stacks.iop.org/Nano/22/485502/mmedia):

$$\begin{aligned} k_{\text{int}} = {} & \{A(\omega_j^2 Q F_{\text{i}} - \tilde{Y}\omega_j \omega k_j) \sin\tilde{\phi} + A Q_j \omega_j^2 F_{\text{r}} \cos\tilde{\phi} \\ & + \omega_j^2 Q_j \tilde{Y} F_{\text{r}} + Q_j k_j (A^2 + A\tilde{Y})(\omega^2 - {\omega_j}^2)\} \\ & \{\omega_j^2 Q_j (2A\tilde{Y}\cos\tilde{\phi} + \tilde{Y}^2 + A^2)\}^{-1} \end{aligned} \tag{13}$$

$$\begin{aligned} \gamma = {} & -\{A Q_j (\tilde{Y}\omega^2 k_j - \tilde{Y}\omega_j^2 k_j - \omega_j^2 F_{\text{r}} A) \sin\tilde{\phi} \\ & + A(\tilde{Y}\omega_j \omega k_j + \omega_j^2 Q_j F_{\text{i}}) \cos\tilde{\phi} + \omega_i^2 Q_j \tilde{Y} F_{\text{i}} \\ & + \omega_j \omega A^2 k_j\} \{\omega_j^2 \omega Q_j (2A\tilde{Y}\cos\tilde{\phi} + \tilde{Y}^2 + A^2)\}^{-1} \end{aligned} \tag{14}$$

where F_{r} and F_{i} are the real and imaginary parts of F from (12). Note that these formulae are only valid when the total tip motion (including the base motion) is small, not necessarily when the observed relative amplitude is small. These formulae are valid in both standard tapping mode (constant excitation) and in constant-amplitude mode (where A is kept constant by adjusting Y).

Finally, the expressions are valid only when the interaction stiffness k_{int} is significantly less than the interaction stiffness on the sample where the residual amplitude was calculated. In other words, the assumption of section 3.2 is that the calibration sample is infinitely stiff. This is a reasonable assumption when k_{int} is significantly softer than the calibration sample.

There also large and arbitrary amplitude AM-AFM force spectroscopy formulae (e.g. [28–30]) which could potentially be modified to include the effects of base motion and fluid-borne loading, although we do not attempt that here.

[6] It is also possible to calculate the true cantilever phase ϕ_0 from (10) prior to the experiment and then use this value to remove the instrumental phase offsets.

5.3. Experimental demonstration

We now demonstrate the use of the proposed small-amplitude force spectroscopy equations (13) and (14) using AM-AFM. The sample studied is octamethylcyclotetrasiloxane (OMCTS), a non-polar, nearly spherical molecule on a mica substrate. OMCTS has been well studied in the AFM literature ([31–34]) and is known to layer near solid surfaces, giving rise to oscillations in the tip–sample forces [35] that have a period of approximately one molecule diameter (∼8 Å). In particular some groups have used small-amplitude piezo-excited AM-AFM to study OMCTS [5, 36], making it a relevant demonstration sample for this theory. The OMCTS (Sigma Aldrich) was dried for several days using 4 Å molecular sieves (Mallinckrodt Chemicals) prior to measurement. An Agilent 5500 AFM with a Mikromasch NSC36 cantilever (Nat. freq = 40.4 kHz, $Q = 2.6$, $k = 1.54$ N m^{-1} by the thermal method) was driven at a free oscillation amplitude of 1.7 Å at a frequency of 27.1 kHz.

The results are shown in figure 4. The raw amplitude and phase is shown in figure 4(a). The results are plotted versus the mean gap, which is $d = Z + M$, where M is the mean deflection[7]. The mean deflection is often neglected in the literature. The $d = 0$ point is chosen to be the point at which the mean deflection is minimum. From these curves A_{fluid} is calculated to be $0.72 + 0.08\mathrm{i}$.

In figure 4(b) the interaction stiffness k_{int} versus mean gap is shown for the two theories. The stiffness is not plotted left of $d = 0$ as the formulae are not valid once the tip enters permanent contact with the substrate (see section 5.2). The line labeled 'ideal theory' shows the results according to the formulae presented in [5]. The new theory is (13) and (14). The results are similar far from the sample, but the theories diverge closer to the sample. In fact, at the very last shell before the surface they are completely different. When approaching the sample, the tip amplitude is decreasing but the base motion is constant. Therefore, accurate knowledge of the base motion becomes increasingly more important as the tip approaches closer to the sample. In figure 4(c) the integrated force $F(d) = \int_d^\infty k_{\text{int}}(x)\,\mathrm{d}x$ from the two theories is shown and this is compared to the mean force (i.e. mean deflection times stiffness). The new theory is close to the mean force, as expected, but the previous theory is not. Finally, in figure 4(d) the damping is shown. Again, the two theories are similar far from the sample but diverge close to the sample.

Note that figure 4(c) shows a net overall repulsive force. This may be indicative of a trace amount of water remaining in the OMCTS sample [35].

6. Discussion

6.1. Frequency dependence: the forest of peaks

This work has made little mention of the 'forest of peaks' [14, 1] caused by piezo resonances and liquid cell

[7] A more typical case would be to plot versus minimum gap $d = Z + M - A_{\text{tot}}$, where A_{tot} is the total amplitude (tip motion plus base motion). But because the two theories make different predictions for A_{tot}, mean gap makes for an easier comparison.

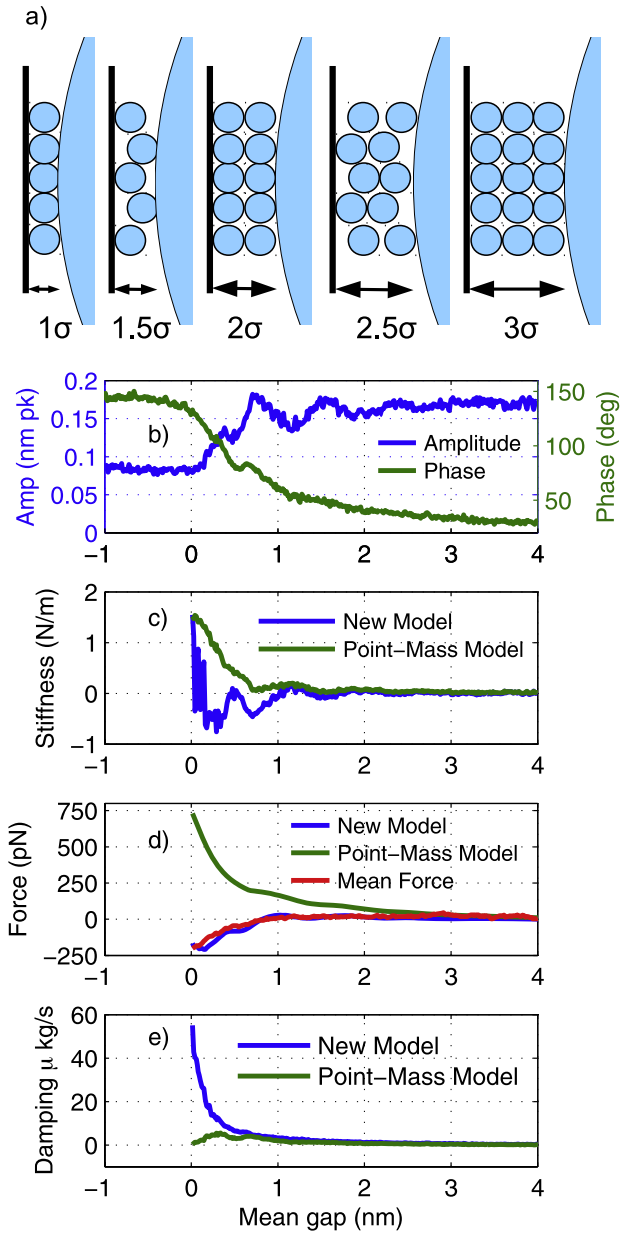

Figure 4. Small-amplitude AM-AFM force spectroscopy on OMCTS solvation shells over mica. (a) Schematic showing confinement-induced ordering in liquid between solid surfaces as the gap is changed (σ is the molecular diameter). This gives rise to oscillations in the liquid density and thus tip–sample force (after [39]). (b) Raw amplitude and phase. (c) Calculated stiffness comparing the previous models [11, 5] to the new model proposed in this work (note: the phase is shifted differently for each theory according to the discussion in section 5.2). (d) Calculated force (integrated from stiffness in (c)) compared to the experimentally measured mean force. (e) Calculated damping comparing the previous models to the new model proposed in this work.

resonances, which has been the subject of many articles. In fact, in AM-AFM or PM-AFM (phase modulation), the drive frequency stays at a fixed frequency during the entire experiment. Therefore the presence of piezo resonances is not necessarily a barrier to quantitative force spectroscopy. The only difficulty it poses is in identifying the natural frequency and quality factor to use in the equations given in this work.

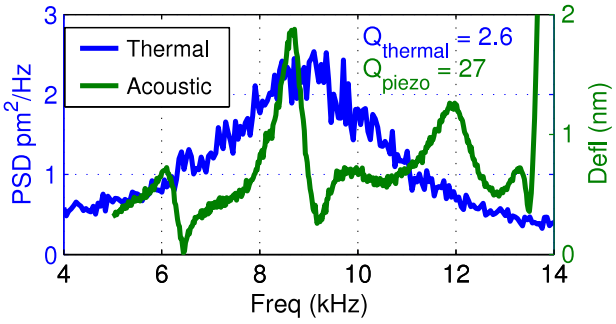

Figure 5. Comparison of thermally driven and piezo-driven spectra for a typical cantilever (Mikromasch CSC37, $k = 0.37$ N m^{-1}) in water, taken in an Agilent 5500 AFM.

Figure 5 shows that the apparent quality factor is different in the thermally driven spectrum than in the piezo-driven spectrum. These apparent quality factors in the driven spectrum are related to the piezo (and mechanical components such as the chip holder) and not to the cantilever. Thus Q must be determined from a thermally driven spectrum. Also, due to the low quality factors in liquid, shortcuts such as determining the natural frequency from the peak of the spectrum, and determining the quality factor from the half-power bandwidth are not accurate. A curve-fitting procedure must be used. In other words, fit the observed power spectral density (in m^2 Hz^{-1}) to $S_0 + S_1 H^2(\omega/\omega_1, Q_1)$, where the fitting parameters are a background noise floor S_0, a scalar S_1, natural frequency ω_1 and quality factor Q_1 and the transfer function is defined as $H(\omega/\omega_j, Q_j) = 1/(1 + \frac{\mathrm{i}}{Q_j}\frac{\omega}{\omega_j} - (\frac{\omega}{\omega_j})^2)$. Then the drive frequency can simply be set to the piezo resonance closest to the cantilever resonance[8]. Researchers should keep in mind that the base motion and fluid-borne excitation may vary from one piezo resonance peak to another, but once these are determined that should not cause further trouble.

However, for frequency modulation AFM, the 'forest of peaks' can cause significant problems, and removing the piezo resonances is necessary (but not sufficient) for quantitative AFM. This result is detailed in a recent paper [37].

Researchers who attempt to build better piezo actuators in order to reduce the forest of peaks (such as [7–10]) must be cautioned that even the complete removal of all piezo resonances is not sufficient to enable quantitative AFM (either AM or FM). The fluid-borne excitation and large base motion will still be present regardless of whether piezo resonances are present.

6.2. *Off-resonant operation*

This paper has focused on operation near resonance (either the fundamental eigenmode or a higher one). Some groups have utilized excitation very far below resonance (for example [36]).

[8] Or even a closer frequency. Despite the fact that most researchers are conditioned to pick the drive frequency at a peak in the excitation spectrum, it is not required to drive exactly at a piezo resonance. One can pick a frequency that is closer to the cantilever resonance, so long as sufficient response amplitude is achieved.

Operation far below resonance should avoid some of the difficulties discussed in this paper because the influence of fluid-borne excitation is expected to be small. However, such non-resonant operation is generally possible only with fiber optic interferometer detection schemes, which are able to measure the cantilever tip displacement directly. The primary problem with fluid-borne excitation arose from the photodiode's inability to measure base motion. Therefore, for groups which possess interferometers or other direct measurement systems, the choice of resonant versus non-resonant operation will not be strongly influenced by fluid-borne excitation concerns.

6.3. Uncertainty

This work has, for the first time, provided an experimentally validated equation for quantitative force and dissipation spectroscopy when using piezo excitation in liquids. Once the base motion is known, (13) and (14) (or their counterparts for other modes) will be just as accurate as the expression for magnetic excitation. However, some additional uncertainty has been introduced in the estimate of the base motion from (10) and (11). Therefore, in AFMs which use a traditional optical beam deflection method and photodiode, direct excitation methods such as magnetic, Lorentz force or photothermal will avoid the uncertainty associated with estimating the base motion. Interferometer-based AFMs [36, 38] could directly measure the base motion, so the methods should be equivalent using those instruments.

6.4. Influence of AFM system used

Researchers with various different AFM configurations will be interested to know if fluid-borne excitation is significant in their systems. This can be simply tested by performing an AM-AFM approach curve on a hard surface and following the procedure in section 3.2. This will yield a complex value of A_{fluid}. If the magnitude of A_{fluid} is greater than about 0.05, then fluid-borne excitation is significant and should not be neglected.

In total, we have performed measurements on three different commercial AFM liquid cells (Nanotec, Agilent, Asylum) and one custom-built liquid cell. All four liquid cells showed significant amounts of fluid-borne excitation, indicating that this a general effect in AFM and is not limited to one specific manufacturer.

7. Summary

In summary, we have demonstrated that accurate knowledge of the base motion in piezo-excited AFM is necessary for quantitative force or dissipation spectroscopy in liquid because the large base motion can alter the observed amplitude and phase through the base–sample work terms. Large base motion is present regardless of the presence or absence of the 'forest of peaks'. We have shown that the actual base motion in piezo-excited AFM in liquids is typically smaller than predicted by previous formulae. This point had been missed by the AFM community for many years because the base motion is not directly observable in typical AFMs and there was no way to confirm or refute the previous theories. Our experiment utilized a scanning laser Doppler vibrometer that was able to directly determine the base motion. From these observations, we have confirmed that there is a force acting on the cantilever transmitted from the piezo through the unsteady motion of the surrounding fluid (fluid-borne excitation), in addition to the mechanical excitation of the base (structure-borne excitation).

We have demonstrated a method to accurately estimate the base motion and fluid-borne loading, and validated it with laser Doppler vibrometer measurements. This new method does not require any additional hardware.

Finally, we formulated small-amplitude force spectroscopy equations based on the new theory and demonstrated them on a representative sample. The results show that force spectroscopy equations based on the previous theory have significant errors due to the inaccurate assumptions about the magnitude of the base motion. Further, the fluid-borne excitation can affect the phase of the response. Thus, without accurate knowledge of the fluid-borne loading, it may not be possible to remove instrumental phase offsets that can cause significant errors in force spectroscopy.

The new proposed method will allow researchers to obtain significantly more accurate measurements in liquids using their existing AFM hardware.

Acknowledgments

The authors would like to thank J Melcher, A Labuda, J Chevrier and K Kobayashi for helpful discussions on this topic, as well as financial support from the National Science Foundation through grant no. CMMI-0927648.

References

[1] Putman C, Werf K, Grooth B, Hulst N and Greve J 1994 *Appl. Phys. Lett.* **64** 2454–6
[2] Han W and Lindsay S M 1996 *Appl. Phys. Lett.* **69** 4111–3
[3] Buguin A, Du Roure O and Silberzan P 2001 *Appl. Phys. Lett.* **78** 2982
[4] Kiracofe D, Kobayashi K, Labuda A, Raman A and Yamada H 2010 *Rev. Sci. Instrum.* **82** 013702
[5] deBeer S, Ende D and Mugele F 2010 *Nanotechnology* **21** 325703
[6] Maali A, Cohen-Bouhacina T and Kellay H 2008 *Appl. Phys. Lett.* **92** 053101
[7] Maali A, Hurth C, Cohen-Bouhacina T, Couturier G and Aimé J 2006 *Appl. Phys. Lett.* **88** 163504
[8] Asakawa H and Fukuma T 2009 *Rev. Sci. Instrum.* **80** 103703
[9] Carrasco C, Ares P, de Pablo P J and Gómez-Herrero J 2008 *Rev. Sci. Instrum.* **79** 126106
[10] Motamedi R and Wood-Adams P 2008 *Sensors* **8** 5927–41
[11] Jai C, Cohen-Bouhacina T and Maali A 2007 *Appl. Phys. Lett.* **90** 113512
[12] Herruzo E and García R 2007 *Appl. Phys. Lett.* **91** 143113
[13] Xu X and Raman A 2007 *J. Appl. Phys.* **102** 034303
[14] Schäffer T E, Cleveland J P, Ohnesorge F, Walters D A and Hansma P K 1996 *J. Appl. Phys.* **80** 3622–7
[15] Chen G Y, Warmack R J, Huang A and Thundat T 1995 *J. Appl. Phys.* **78** 1465–9
[16] O'Shea S J and Welland M E 1998 *Langmuir* **14** 4186–97
[17] Anczykowski B, Gotsmann B, Fuchs H, Cleveland J P and Elings V B 1999 *Appl. Surf. Sci.* **140** 376–82

[18] Melcher J, Hu S and Raman A 2007 *Appl. Phys. Lett.* **91** 53101
[19] Kiracofe D and Raman A 2010 *J. Appl. Phys.* **107** 3506
[20] Lozano J R, Kiracofe D, Melcher J, Garcia R and Raman A 2010 *Nanotechnology* **21** 465502
[21] Sader J E and Jarvis S P 2004 *Appl. Phys. Lett.* **84** 1801–3
[22] Volkov A, Burnell-Gray J and Datta P 2004 *Appl. Phys. Lett.* **85** 5397
[23] Sader J E 1998 *J. Appl. Phys.* **84** 64–76
[24] Tuck E O 1969 *J. Eng. Math.* **3** 44
[25] Lantz M, Liu Y Z, Cui X D, Tokumoto H and Lindsay S M 1999 *Surf. Interface Anal.* **27** 354–60
[26] https://nanohub.org/resources/abase
[27] Spletzer M, Raman A and Reifenberger R 2010 *J. Micromech. Microeng.* **20** 085024
[28] Hu S and Raman A 2008 *Nanotechnology* **19** 375704
[29] Katan A, van Es M and Oosterkamp T 2009 *Nanotechnology* **20** 165703
[30] Holscher H 2006 *Appl. Phys. Lett.* **89** 123109
[31] O'Shea S 2001 *Japan. J. Appl. Phys.* **40** 4309–13
[32] Kaggwa G B, Kilpatrick J I, Sader J E and Jarvis S P 2008 *Appl. Phys. Lett.* **93** 011909
[33] Uchihashi T, Higgins M, Nakayama Y, Sader J and Jarvis S 2005 *Nanotechnology* **16** 49
[34] Han W and Lindsay S 1998 *Appl. Phys. Lett.* **72** 1656
[35] Horn R G and Israelachvili J N 1981 *J. Chem. Phys.* **75** 1400–11
[36] Patil S, Matei G, Dong H and Hoffmann P M 2005 *Rev. Sci. Instrum.* **76** 103705
[37] Labuda A, Kobayashi K, Kiracofe D, Suzuki K, Grütter P and Yamada H 2011 *AIP Adv.* **1** 022136
[38] Jourdan G, Lambrecht A, Comin F and Chevrier J 2009 *Europhys. Lett.* **85** 31001
[39] Israelachvili J 1992 *Intermolecular and Surface Forces* 2nd edn (New York: Academic)